Cell Reports, Volume *16*

Supplemental Information

Kinetics of Spontaneous and EF-G-Accelerated Rotation of Ribosomal Subunits

Heena Sharma, Sarah Adio, Tamara Senyushkina, Riccardo Belardinelli, Frank Peske, and Marina V. Rodnina

SUPPLEMENTAL FIGURES

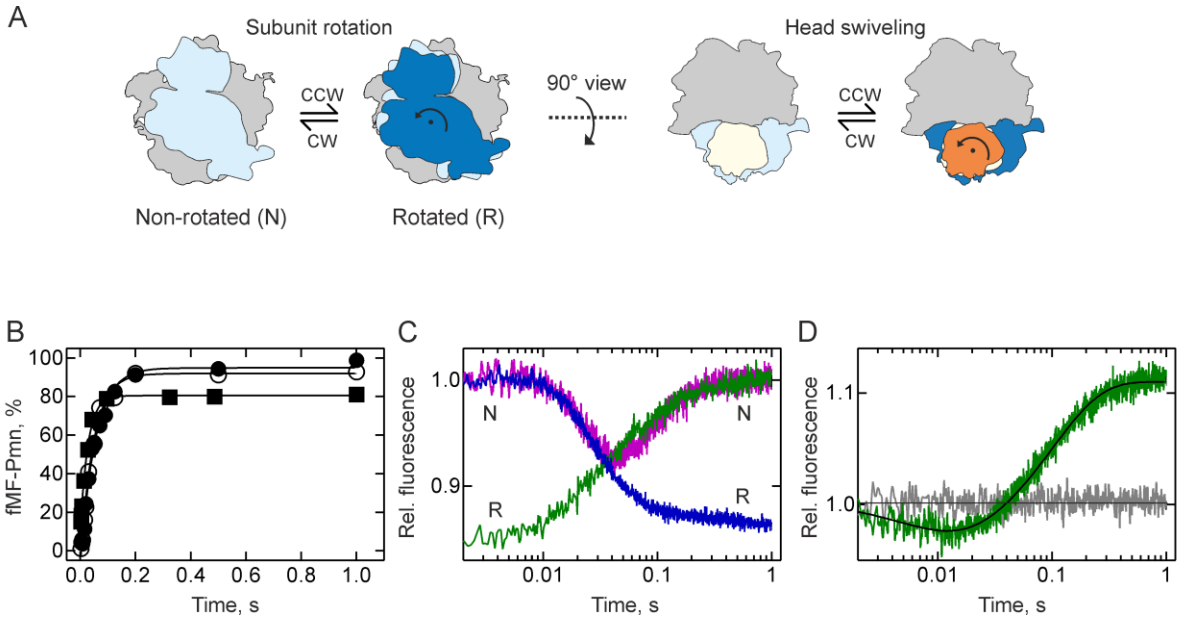

Figure S1. Characterization of bS6-bL9 Double-Labeled Ribosomes, Related to Figure 1

(A) Dynamic modes of subunit motions. The rotation states of the SSU relative to the LSU (gray) are indicated by color intensity of the SSU body (light blue for N, dark blue for R). The swiveling motions of the SSU head are shown by color change from light yellow (classical non-swiveled SSU head position) to orange (maximum degree of swiveling relative to the SSU body).
(B) Time resolved Pmn assay for the wild type (closed circle), labeled (S6Alexa488-L9Alexa568) (open circles) and labeled (S6Cy5-L9Cy3) (closed squares) ribosomes.
(C) FRET changes (monitored by fluorescence change of acceptor) upon addition of the ternary complex EF-Tu–GTP–Phe-tRNA^{Phe} to the initiation complex 70S–mRNA–fMet-tRNA^{fMet}, which results in the formation of the PRE complex in the rotated state (blue). Addition of EF-G to the rotated PRE complex forms the POST complex (green). Initiation complex was mixed with ternary complex and EF-G together (pink).
(D) FRET change in the PRE(fMV) complex upon addition of EF-G and translocation (green) or upon mixing with buffer in the absence of EF-G (grey).

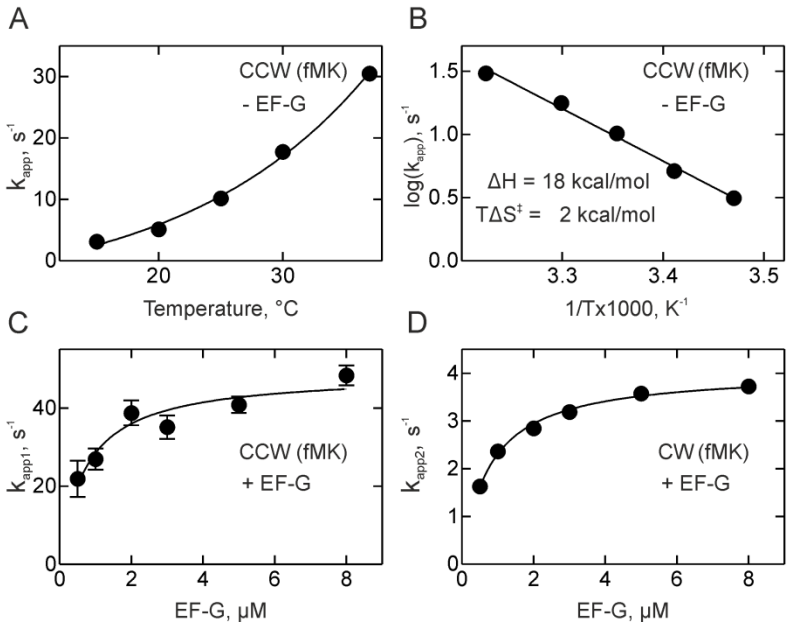

Figure S2. Temperature Dependence of Subunit Rotation, Related to Figures 1 and 4 and Tables 2 and S1

(A and B) Temperature dependence of the spontaneous CCW subunit rotation upon reaction of fMK with Pmn.
(C and D) EF-G concentration dependence of the apparent rate constants of subunit rotation for PRE(fMK) at 25°C. Hyperbolic fits saturate for the CCW rotation at $k_{app1} = 50 \pm 3\ s^{-1}$ with K_M of 0.7 ± 0.2 μM and for the CW rotation at $k_{app2} = 4.0 \pm 0.1\ s^{-1}$ with K_M of 0.8 ± 0.1 μM. Error bars are mean values with s.e.m. of the fit.

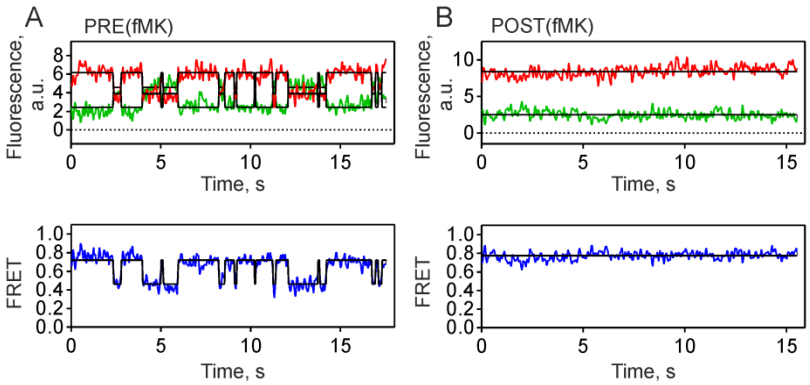

Figure S3. smFRET in the PRE(fMK) Complex, Related to Figure 3 and Tables 1 and Table S1

Representative examples of single-molecule fluorescence intensity trajectories for Cy3 (green) and Cy5 (red) (top panel), and the trajectory of FRET over time (lower panel) (A) in PRE complex and (B) in POST complex

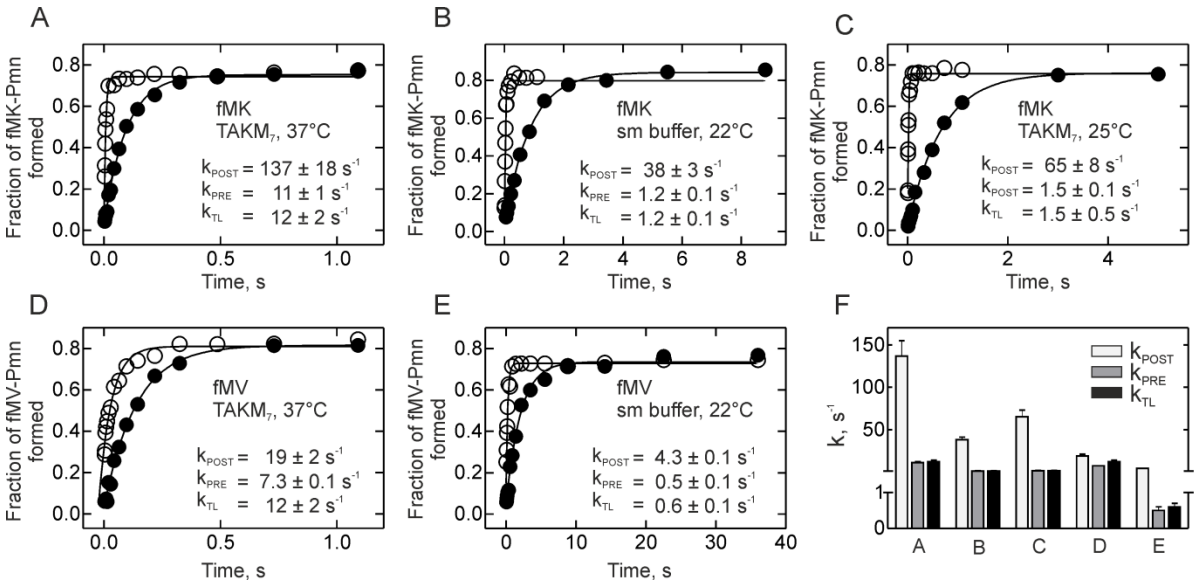

Figure S4. Time-Resolved Pmn Reaction to Determine the Rate of Translocation, Related to Figure 4 and Table 2

Open symbols, Pmn reaction with POST complexes; closed symbols, Pmn reaction with PRE complexes upon addition of EF-G. Reaction rates in the POST and PRE complexes were estimated by exponential fitting. k_{TL} was calculated from k_{POST} and k_{PRE} as described in Supplemental Experimental Procedures.

(A) fMK complexes in $TAKM_7$ at 37°C.

(B) fMK complexes in smFRET buffer at 22°C.

(C) fMK complexes in $TAKM_7$ at 25°C.

(D) fMV complexes in $TAKM_7$ at 37°C.

(E) fMV complexes in smFRET buffer at 22°C.

(F) Summary of the rate constants from panels A-E.

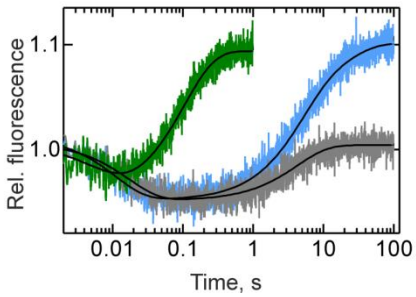

Figure S5. Role of GTP Hydrolysis, Related to Figure 4

FRET change upon reaction of PRE(fMV) complex with EF-G–GTP (green), EF-G–GTPγS (grey), or a mutant EF-G(H583K)–GTP (blue) which is known to be slow in translocation (Savelsbergh et al., 2000).

Table S1. Fraction of N State in PRE Complexes, Related to Figures 3 and 4

PRE	Experimental conditions			
	22°C		25°C	37°C
	smFRET[a]	sm buffer[b]	$TAKM_7$[b]	$TAKM_7$[b]
fMK	0.69 ± 0.03 (512)[c]	0.60 ± 0.04	0.44 ± 0.01	0.41 ± 0.02
fMV	0.60 ± 0.05 (335)[c]	0.57 ± 0.01	n.d.	0.35 ± 0.01
fMF	0.48 ± 0.01 (467)[c]	n.d.	n.d.	0.12 ± 0.03

[a] Determined from the population distribution of smFRET experiment. N is the population in high-FRET state (FRET efficiency = 0.7); R is the population in low-FRET state (FRET efficiency = 0.5).
[b] Calculated from the relative amplitudes of the CCW to CW rotations from ensemble kinetics.
[c] The number of traces used to construct the state distribution histograms.
Values are mean ± s.d. from 3 independent data sets.

Table S2. Spontaneous and EF-G-Induced Transitions in the PRE Complex, Related to Figures 1-4 and Note S1

SUPPLEMENTAL EXPERIMENTAL PROCEDURES

Ribosomes, mRNAs, tRNAs and translation factors

The chromosomal genes for proteins L9 (*rplI*) and S6 (*rpsF*) were deleted in *E. coli* strain BW25113 using the Quick & Easy *E. coli* Gene Deletion Kit (Gene Bridges). The deletion of the genes was confirmed on both the DNA level using gene-specific PCR primers and on the protein level by western blotting and mass spectrometry. Ribosomal subunits were prepared from the deletion strains (ΔL9 and ΔS6) according to the protocol used for native ribosomes (Rodnina and Wintermeyer, 1995). Initiation factors (IF1, IF2, IF3), EF-G, EF-Tu and tRNAs (f[^{3}H]Met-tRNA^{fMet} [^{14}C]Lys-tRNA^{Lys}, [^{14}C]Val-tRNA^{Val}, [^{14}C]Phe-tRNA^{Phe}, [^{14}C]Pro-tRNA^{Pro}) were prepared as described (Cunha et al., 2013a; Holtkamp et al., 2014; Rodnina and Wintermeyer, 1995; Savelsbergh et al., 2003). The following mRNA constructs (IBA, Göttingen) were used (start codon and first elongation codon are underlined).

For stopped-flow experiments and time resolved Pmn assays:

mMK: GUUAACAGGUAUACAUACU<u>AUGAAA</u>UUCAUUAC
mMV: GUUAACAGGUAUACAUACU<u>AUGGUG</u>UUCAUUAC
mMF: GUUAACAGGUAUACAUACU<u>AUGUUU</u>GUUAUUAC
mMP: GGCAAGGAGGUAAAUA<u>AUGCCG</u>UUCAUU

For smFRET experiments (mRNAs were biotinylated at the 5' end for attachment to the quartz surface (Adio et al., 2015; Blanchard et al., 2004)):

mMK: CAACCUAAAACUUACACACCCGGCAAGGAGGUAAAUA<u>AUGAAG</u>UAAACGAUU
mMV: CAACCUAAAACUUACACACCCGGCAAGGAGGUAAAUA<u>AUGGUU</u>UAAACGAUU
mMF: CAACCUAAAACUUACACACCCGGCAAGGAGGUAAAUA<u>AUGUUC</u>UAAACGAUU

Labeling of ribosomal subunits

E. coli genes for proteins bL9 and bS6 were PCR-amplified from strain BW25113 and cloned individually into the pET28(a) plasmid (Novagen). Both proteins do not contain native cysteines. For site-specific fluorescence labeling, cysteines were introduced by site-directed mutagenesis at position 41 in protein bS6, replacing aspartic acid, and at position 11 in protein bL9, replacing asparagine. Expression, purification and refolding of proteins were performed essentially as described (Ermolenko et al., 2007; Hickerson et al., 2005; Lieberman et al., 2000). Labeling was performed under denaturing conditions in buffer (50 mM HEPES (pH 7.3), 400 mM KCl, 6 M urea) at 4°C overnight, and the reaction was quenched with 6 mM 2-mercaptoethanol. Excess free dye was removed by gel filtration on a Superdex 75 10/300 GL column (GE Healthcare); the absence of free dye was confirmed by SDS-PAGE. The proteins were refolded by stepwise dialysis into buffer (50 mM HEPES (pH 7.5), 400 mM KCl, 4 mM $MgCl_2$, 5%, v/v, glycerol).

Purified ΔS6 SSU were reconstituted with a 2-fold molar excess of Alexa 488- or Cy5-labeled protein bS6 in buffer (50 mM HEPES (pH 7.5), 400 mM KCl, 20 mM $MgCl_2$, 5%, v/v, glycerol) at 42°C for 60 min. Similarly, purified ΔL9 LSU were reconstituted with a 2-fold molar excess of Alexa 568- or Cy3-labeled protein bL9 in buffer (50 mM HEPES (pH 7.5), 400 mM NH_4Cl, 4 mM $MgCl_2$, 5% v/v glycerol) at 37°C for 60 min. Reconstituted subunits were purified by centrifugation through a 30% sucrose cushion in $TAKM_7$ buffer (50 mM Tris-HCl (pH 7.5), 70 mM NH_4Cl, 30 mM KCl, 7 mM $MgCl_2$) to remove excess labeled protein. The extent of subunit labeling determined spectroscopically was close to 100%, assuming extinction coefficients of 73,000 $cm^{-1}M^{-1}$ for Alexa 488, 88,000 $cm^{-1}M^{-1}$ for Alexa 568, 150,000 $cm^{-1}M^{-1}$ for Cy3 and 250,000 $cm^{-1}M^{-1}$ for Cy5. Subunit concentrations were determined by absorption measurements at 260 nm on the basis of 67 pmol/A260 unit for SSU and 37 pmol/A260 unit for LSU (Richter, 1976).

Preparation of the complexes

Preparation and purification of initiation, PRE and POST complexes were carried out as described (Belardinelli et al., 2016; Cunha et al., 2013b; Holtkamp et al., 2014; Rodnina et al., 1997). Briefly, labeled SSU were first heat activated in TAKM with 21 mM $MgCl_2$ for 30 min at 37°C, combined with a 1.5-fold excess of labeled LSU and incubated with a 3-fold excess of mRNA and a 2-fold excess of IF1, IF2, IF3 each and a 2.5-fold excess of f[^{3}H]Met-tRNA^{fMet} in $TAKM_7$ buffer containing 1 mM GTP for 30 min at 37°C. Initiation complexes were purified through 1.1 M sucrose cushion in $TAKM_7$. Ternary complexes EF-Tu–GTP–X-tRNA^X (X is Lys, Val, Phe or Pro) were prepared by incubating EF-Tu (2-fold excess over tRNA) with 1 mM GTP, 3 mM phosphophenolpyruvate and 0.1 mg ml^{-1} pyruvate kinase for 15 min at 37°C prior to the addition of aa-tRNA. PRE complex was formed by mixing initiation complexes with a 2-fold excess of ternary complex and incubated for 1 min at 37°C. The resulting

PRE complexes were purified by centrifugation through 1.1 M sucrose cushion in TAKM containing 21 mM $MgCl_2$. The pellets were resuspended in the same buffer and the amount of aa-tRNA binding was measured by nitrocellulose filtration. POST complexes were prepared by adding EF-G (5 nM) to the PRE complexes with 1 mM GTP and incubating for 1 min at 37°C.

Rapid kinetics

Subunit rotation experiments were carried out using a stopped-flow apparatus (SX-20MV; Applied Photophysics) in $TAKM_7$ at 37°C, unless otherwise specified. To monitor subunit rotation we used double-labeled ribosomes (S6Alexa488–L9Alexa568). Alexa 488 was excited at 470 nm and fluorescence of Alexa 568 was monitored after passing through a OG590 cut-off filter (Schott). Spontaneous subunit rotation was monitored by mixing equal volumes of purified POST or initiation complexes (0.1 µM) with either Pmn (10 mM) or ternary complexes (10 µM). Rates of peptide bond formation were measured in a quench-flow apparatus (KinTek). Initiation or POST complexes (0.1 µM) were rapidly mixed with Pmn (10 mM) or ternary complexes (10 µM) and the reaction was quenched with KOH (0.8 M). Peptides were released by alkaline hydrolysis for 45 min at 37°C and analyzed by reversed phase HPLC (LiChrospher 100 RP-8, Merck) and quantified by radioactivity counting (Wohlgemuth et al., 2008).

The concentration dependence of peptide bond formation and the spontaneous subunit rotation with fMK complex (0.1 µM) was performed upon addition of increasing concentrations of Pmn (0.1–20 mM) in either stopped-flow or quench-flow experiments. The temperature dependence of spontaneous subunit rotation was measured with the PRE(fMK) complex (0.1 µM) and Pmn (10 mM) at 15, 20, 25, 30, and 37°C by stopped-flow. Time courses for EF-G-induced subunit rotation were monitored after rapidly mixing PRE complexes (0.05 µM) with EF-G (4 µM) in a stopped-flow apparatus in $TAKM_7$ at 37°C or 25°C, as indicated, or in smFRET buffer (see below) at 22°C. The concentration dependence of subunit rotation for PRE(fMK) and PRE(fMV) (0.05 µM) complexes was monitored with increasing concentration of EF-G (0.5 - 8 µM) in $TAKM_7$ at 37°C and 25°C. Time courses of subunit rotation was also measured with PRE(fMV) complex (0.05 µM) in the presence of EF-G (4 µM) and GTP (1 mM) or GTPγS (1 mM); or EF-G(H583K) (4 µM) and GTP (1 mM) in $TAKM_7$, 37°C.

Time-resolved Pmn assay

The functional activity of ribosome complexes was verified by the time-resolved Pmn assay (Holtkamp et al., 2014). Briefly, fluorescence-labeled or non-labeled PRE(fMF) complexes (0.2 µM final concentration) were rapidly mixed in the quench-flow apparatus with Pmn (10 mM), EF-G (4 µM), and GTP (1 mM). The reaction was quenched with 50% formic acid and samples were treated with 1.5 M sodium acetate saturated with $MgSO_4$. f[^{3}H]Met[^{14}C]Phe-Pmn was extracted into ethyl acetate and quantified by double-label radioactivity counting.

To determine the rate of translocation for PRE(fMK) and PRE(fMV) complexes, PRE or POST complexes (0.2 µM) were mixed with Pmn (10 mM) and EF-G (4 µM) or Pmn (10 mM) in $TAKM_7$ at 37°C, in smFRET buffer at 22°C, or in $TAKM_7$ at 25°C. The reaction was quenched with KOH (0.5 M) and the peptides were released by alkaline hydrolysis for 45 min at 37°C, analyzed by reversed-phase HPLC (LiChrospher 100 RP-8, Merck), and quantified by double-label radioactivity counting (Wohlgemuth et al., 2008). The time required for the PRE complex to react (apparent rate constant k_{PRE}) includes the time needed for translocation ($1/k_{TL}$) and for the Pmn reaction of the resulting POST state ($1/k_{POST}$). Deconvolution of the translocation rate from the two values ($k_{TL} = k_{PRE} \times k_{POST} / (k_{PRE} - k_{POST})$ gives the rate of tRNA translocation (Holtkamp et al., 2014).

Data analysis

Exponential fitting was performed using GraphPad Prism. Time courses of peptide bond formation (**Figures 1A, 1D, 2A, S1B and S4**) were evaluated by single-exponential fitting. Time courses of CCW rotation after the Pmn reaction (**Figures 1B, 1E, S2A and S2B)** were initially evaluated by an equation accounting for one (fMV) or two (fMK, fMF) exponential terms after a delay due to the preceding Pmn reaction. The origin of the minor additional downward phase is unknown; it constituted 12% and 20% of the total signal for fMK and fMF complexes, respectively. The elemental rate of subunit rotation for fMK ($k_{CCW} = 48 \pm 3\ s^{-1}$) was calculated from $k_{pep} = 240 \pm 20\ s^{-1}$ **(Figure 1D)** and $k_{rot} = 40 \pm 1\ s^{-1}$ **(Figure 1E)** using the equation $k_{CCW} = k_{pep} \times k_{rot} / (k_{pep} - k_{rot})$. Time courses with fMP did not show the delay and were evaluated by two-exponential fitting with the two phases constituting 55% and 45% of the total amplitude change.

Time courses of EF-G-catalyzed subunit rotation with PRE(fMK) and PRE(fMV) (at all conditions) and with PRE(fMF) at smFRET conditions (**Figures 4, S2C and S2D**) were evaluated by two-exponential fitting. From the two exponential fitting of the traces for PRE(fMK) and PRE(fMV) the ratio of the amplitude change for the downward phase (A_1) and upward phase (A_2) was calculated. The downward phase A_1 represents the CCW rotation

on those ribosomes that were in the N state before EF-G addition. The upward phase A_2 provides the full span of the R to N transitions on all ribosomes. Thus, the A_1/A_2 ratio gave the fraction of the ribosome in the N state before EF-G binding.

Numerical integration analysis was carried out with KinTek Explorer (Johnson et al., 2009) using a two- or three-step model, as was required, with all steps irreversible for the traces in **Figures 1A and 1B**. The first two steps describe the formation of the peptide bond and the subsequent the subunit rotation, respectively. We assumed that the subunit rotation is quasi-irreversible at 37°C in $TAKM_7$. The third step is to account for a slow decrease at the end of each stopped-flow trace (see above). From the analysis we obtained the rate constant of peptide bond formation and the elemental rate of subunit rotation as reported in **Figure 1F**. For fMP, numerical integration analysis with a two-step model was unable to deconvolute the steps of subunit rotation and peptide bond formation. The apparent rate constants of the first and the second steps were about 0.2 s^{-1} and 0.03 s^{-1} respectively, which were the same as the rates from exponential fitting, precluding further analysis.

Numerical integration was also performed for the data shown in **Figures 2A–C** using three-step and two-step models (no slow phase was observed for the complexes shown in Figure 2C), respectively. We noted that for POST(fMF) complex **(Figure 2C**), there was a maximum change in the amplitude for N to R transition upon binding of ternary complex and the final intrinsic florescence intensity (IFI) value was the smallest compared to other complexes **(Figure 2B).** We assumed, in the simplest model, that the endpoint differences between the time courses in **Figure 2B** reflect the difference in the fraction of R states in the final population of ribosomes. We thus fixed the absolute IFI value for the R state to that obtained for the POST(fMF) complex. In the three-step model used for fitting, the first irreversible step accounted for peptide bond formation, the second reversible step was the subunit rotation (CCW and CW), and the third step (where necessary) accounted for the additional minor decrease at the end of each stop-flow trace. All data for PRE(fMK), PRE(fMV) and PRE(fMF) complexes, including quench-flow and stopped-flow time courses were fitted simultaneously (global fit) using the same IFI values for the N and R state independently of tRNAs. Average values of rate constants and standard deviations (s.d.) were calculated from three independent experiments.

Single-molecule FRET

smFRET experiments were carried out in smFRET buffer (50 mM Tris-HCl (pH 7.5), 70 mM NH_4Cl, 30 mM KCl, 15 mM $MgCl_2$, 1 mM spermidine and 8 mM putrescine) and data analysis was performed as described (Adio et al., 2015) using double-labeled ribosomes (S6Cy5–L9Cy3). Initiation complexes were formed by incubating ribosomes (0.1 µM) with a 1.7-fold excess of IF1, IF2 and IF3, 3-fold excess of mRNA biotinylated at the 5' end and fMet-$tRNA^{fMet}$, and GTP (1 mM) in $TAKM_7$ at 37°C for 30 min. Ternary complexes were prepared as described above with EF-Tu (1 µM) and X-$tRNA^X$ (X is Lys, Val, Phe) (0.5 µM). Initiation complexes were mixed with a 5-fold excess of ternary complex and incubated for 1 min at room temperature to form PRE complexes. POST complexes were formed by incubating PRE complexes with EF-G (0.1 µM) and GTP (1 mM).

NOTE S1.

Summary of smFRET and ensemble kinetic data on ribosome fluctuations linked to translocation.

Ribosome dynamics plays a key role in EF-G-catalyzed translocation. Some aspects of ribosome dynamics in translocation are extensively studied and well understood. The most commonly studied motions are rotations of the ribosomal subunits (N to R and R to N), swiveling motions of the SSU head, changes of tRNA positions from classical (C) to hybrid (H) position, and closing of the L1 stalk on the E-site tRNA. These motions can occur spontaneously in the absence of EF-G and are only loosely coupled (Fischer et al., 2010; Munro et al., 2010c; Wasserman et al., 2016). smFRET studies provided important insights into spontaneous ribosome dynamics by looking from several perspectives, i.e., using labels at different positions of the ribosome complex. Due to the variety of reporters, experimental conditions, and differences in ribosome complexes under study, it is sometimes difficult to compare the results of individual papers and assess their relevance for understanding translocation. This Supplemental Note and Table S2 are designed to make this information more accessible.

To classify the available experimental information, we first sort them according to the type of ribosome complexes used in the studies, i.e., PRE complexes, complexes with a vacant A site, or and vacant ribosomes lacking both A- and P-site tRNAs (Table S2). Of these three types of complexes, the experiments with PRE complexes are of immediate relevance for understanding translocation, because the occupancy of the A site is a key prerequisite for the reaction (Joseph and Noller, 1998).

Among the experiments with PRE complexes, we then distinguish three major types of movements, subunit rotation, tRNA repositioning and L1 movement (Table S2, sheet 1, and references therein). The subunit rotation from N to R (CCW) and from R to N (CW) was studied by labels attached to ribosomal proteins S6 and L9 (Cornish et al., 2008; Qin et al., 2014), or helices h44 and H101 (Marshall et al., 2008) on the SSU and LSU, respectively. More recently, subunit rotation has also been monitored using a FRET pair on proteins S13 and L1 and S13 and L5 (Wasserman et al., 2016). We note that the assignment of S13-L1 and S13-L5 dynamics as subunit rotation is not unambiguous, as it may also represent movements of the L1 stalk or the SSU head relative to the body. To study tRNA movements from the C to H and H to C states, different groups utilized labels on the tRNAs in the A and P sites (Adio et al., 2015; Blanchard et al., 2004; Chen et al., 2011; Kim et al., 2007; Munro et al., 2007; Munro et al., 2010a; Wasserman et al., 2016). Additionally, the A-site tRNA movement was monitored by a fluorescence reporter pair attached to the tRNA and protein L11 (Adio et al., 2015; Chen et al., 2011), L27 (Altuntop et al., 2010), and S13 (Wasserman et al., 2016). Finally, L1 closing and opening was visualized by L1-tRNA (Fei et al., 2009; Fei et al., 2008; Munro et al., 2010b), L1-L9 (Fei et al., 2009), and L1-L33 pairs (Cornish et al., 2009; Qin et al., 2014).

Spontaneous ribosome transitions in the absence of EF-G are well characterized. Addition of EF-G induces rapid translocation, which makes it difficult to dissect the effect of the factor on the transitions, because PRE complexes are rapidly converted to the POST state. Several smFRET papers identify translocation intermediates (INT or CHI states) (Adio et al., 2015; Chen et al., 2011; Munro et al., 2007; Wasserman et al., 2016); those are not addressed here and in the following we will summarize what is known about the kinetics of spontaneous ribosome dynamics in the absence of EF-G.

For the SU rotation in the CCW direction measured with the S6-L9 reporter, most k_{CCW} values are between 0.3 s^{-1} and 1.7 s^{-1} (Cornish et al., 2008; Qin et al., 2014); these values compare reasonably well with those determined by us, 2-4 s^{-1} (Table 1). An alternative FRET pair S13-L1 reports on a relatively rapid rearrangement, 4.7 s^{-1}, whereas the S13-L5 pair reports on a slower reaction, about 0.1 s^{-1} (Wasserman et al., 2016). With the S6-L9, S13-L1, and S13-L5 labels, the N to R rotation in the PRE complex is reversible with a rate of CW rotation in the range of 0.02 s^{-1} to 12.7 s^{-1} (this paper Table 1, 22°C, and (Cornish et al., 2008; Qin et al., 2014; Wasserman et al., 2016). Surprisingly, when the labels are attached to rRNA (h44-H101), CCW rotation is very slow (about 0.05 s^{-1}) and quasi irreversible (Marshall et al., 2008). The effect of EF-G on the subunit rotation of the PRE complex has not been reported previously, because EF-G addition facilitates rapid formation of translocation intermediates followed by translocation (Wasserman et al., 2016).

Experiments monitoring C-to-H tRNA transitions provide a similar kinetic picture. The rates of C-to-H transitions $k_{C\rightarrow H}$ are in the range from 0.6 to 10 s^{-1} and are reversible with $k_{H\rightarrow C}$ between 0.7 and 4 s^{-1}, and a resulting ratio between H and C states ranging from 0.2 to 2 (Adio et al., 2015; Altuntop et al., 2010; Blanchard et al., 2004; Chen et al., 2011; Kim et al., 2007; Munro et al., 2007; Munro et al., 2010a; Wasserman et al., 2016). Again, the effect of EF-G on the C-to-H transition is difficult to assess, because EF-G induces rapid formation of translocation intermediates that differ from the initial H and C states (Adio et al., 2015; Chen et al., 2011; Wasserman et al., 2016).

Probably the most studied transition is the movement of protein L1 towards or away from the E-site tRNA, which we define as open-to-closed transition. Most of the estimated closing rates $k_{L1open \rightarrow closed}$ are around 2-5 s^{-1} (Cornish et al., 2009; Fei et al., 2009; Munro et al., 2010a; Munro et al., 2010c). The rates of opening $k_{L1open \rightarrow closed}$ are from 0.4 s^{-1} (Cornish et al., 2009) to as high as 46 s^{-1} (Munro et al., 2010c); in the latter case the high observed rate may reflect the existence of intermediates. EF-G addition results in rapid translocation (Fei et al., 2008). In one case, fluctuations between open and closed L1 conformations were observed after EF-G addition and the rate of these transitions was not changed compared to spontaneous transitions in the absence of EF-G (Munro et al., 2010c). However, the exact timing of EF-G arrival to the ribosomes in those experiments remained unclear and it is difficult to rule out a possibility that the observed unaltered fluctuations represent ribosome dynamics in the absence of EF-G. In summary, smFRET measurements suggests that in the PRE complex N to R, C to H and L1 open to closed transitions are spontaneous and reversible, loosely coupled and thermodynamically driven and the effect of EF-G on the rate of these transitions is not clear.

Because the effect of EF-G on PRE complexes is elusive and difficult to resolve, several studies addressed EF-G-induced ribosome dynamics with complexes that lacked a tRNA in the A site or with vacant ribosomes lacking tRNAs in both A and P sites (Table S2, sheet 2). The dynamics of vacant ribosomes or ribosomes with a peptidyl-tRNA in the P site was very slow (Cornish et al., 2008). For the complexes with a vacant A site and a deacylated tRNA in the P site, the rates of fluctuations are similar to those on PRE complexes. The reported acceleration effect of EF-G on the ribosome rotation (measured with S6-L9 pair) was two-fold (Cornish et al., 2008), and on L1 closure six- to eight-fold (Fei et al., 2009; Munro et al., 2010b). Because of the lack of the A-site tRNA, which is essential for translocation (Joseph and Noller, 1998), it is unclear whether these results pertain to the situation during on-going translocation, particularly in view of the absence of the EF-G effect on PRE complexes. We note that despite a large eight-fold effect of EF-G–GDPNP binding on the rate of L1 closure, the authors concluded that EF-G does not accelerate the formation of the R–H–$L1_{closed}$ state (Munro et al., 2010b). In general, the rates obtained by smFRET are significantly slower than those estimated by ensemble kinetics (Table S2, sheet 3). On the other hand, the rate of spontaneous subunit rotation was not measured by ensemble kinetics. This summary illustrates that the effect of EF-G on the subunit rotation prior to translocation is not known, despite a wealth of information on the ribosome dynamics obtained by smFRET.

SUPPLEMENTAL REFERENCES

Adio, S., Senyushkina, T., Peske, F., Fischer, N., Wintermeyer, W., and Rodnina, M.V. (2015). Fluctuations between multiple EF-G-induced chimeric tRNA states during translocation on the ribosome. Nat Commun *6*, 7442.

Altuntop, M.E., Ly, C.T., and Wang, Y. (2010). Single-molecule study of ribosome hierarchic dynamics at the peptidyl transferase center. Biophys J *99*, 3002-3009.

Belardinelli, R., Sharma, H., Caliskan, N., Cunha, C.E., Peske, F., Wintermeyer, W., and Rodnina, M.V. (2016). Choreography of molecular movements during ribosome progression along mRNA. Nat Struct Mol Biol *23*, 342-348.

Blanchard, S.C., Kim, H.D., Gonzalez, R.L., Jr., Puglisi, J.D., and Chu, S. (2004). tRNA dynamics on the ribosome during translation. Proc Natl Acad Sci U S A *101*, 12893-12898.

Chen, C., Stevens, B., Kaur, J., Cabral, D., Liu, H., Wang, Y., Zhang, H., Rosenblum, G., Smilansky, Z., Goldman, Y.E., *et al.* (2011). Single-molecule fluorescence measurements of ribosomal translocation dynamics. Mol Cell *42*, 367-377.

Cornish, P.V., Ermolenko, D.N., Noller, H.F., and Ha, T. (2008). Spontaneous intersubunit rotation in single ribosomes. Mol Cell *30*, 578-588.

Cornish, P.V., Ermolenko, D.N., Staple, D.W., Hoang, L., Hickerson, R.P., Noller, H.F., and Ha, T. (2009). Following movement of the L1 stalk between three functional states in single ribosomes. Proc Natl Acad Sci U S A *106*, 2571-2576.

Cunha, C.E., Belardinelli, R., Peske, F., Holtkamp, W., Wintermeyer, W., and Rodnina, M.V. (2013b). Dual use of GTP hydrolysis by elongation factor G on the ribosome. Translation *1*, e24315.

Ermolenko, D.N., Majumdar, Z.K., Hickerson, R.P., Spiegel, P.C., Clegg, R.M., and Noller, H.F. (2007). Observation of intersubunit movement of the ribosome in solution using FRET. J Mol Biol *370*, 530-540.

Fei, J., Bronson, J.E., Hofman, J.M., Srinivas, R.L., Wiggins, C.H., and Gonzalez, R.L., Jr. (2009). Allosteric collaboration between elongation factor G and the ribosomal L1 stalk directs tRNA movements during translation. Proc Natl Acad Sci U S A *106*, 15702-15707.

Fei, J., Kosuri, P., MacDougall, D.D., and Gonzalez, R.L., Jr. (2008). Coupling of ribosomal L1 stalk and tRNA dynamics during translation elongation. Mol Cell *30*, 348-359.

Fischer, N., Konevega, A.L., Wintermeyer, W., Rodnina, M.V., and Stark, H. (2010). Ribosome dynamics and tRNA movement by time-resolved electron cryomicroscopy. Nature *466*, 329-333.

Hickerson, R., Majumdar, Z.K., Baucom, A., Clegg, R.M., and Noller, H.F. (2005). Measurement of internal movements within the 30 S ribosomal subunit using Forster resonance energy transfer. J Mol Biol *354*, 459-472.

Holtkamp, W., Cunha, C.E., Peske, F., Konevega, A.L., Wintermeyer, W., and Rodnina, M.V. (2014). GTP hydrolysis by EF-G synchronizes tRNA movement on small and large ribosomal subunits. EMBO J *33*, 1073-1085.

Johnson, K.A., Simpson, Z.B., and Blom, T. (2009). Global kinetic explorer: a new computer program for dynamic simulation and fitting of kinetic data. Anal Biochem *387*, 20-29.

Joseph, S., and Noller, H.F. (1998). EF-G-catalyzed translocation of anticodon stem-loop analogs of transfer RNA in the ribosome. EMBO J *17*, 3478-3483.

Kim, H.D., Puglisi, J.D., and Chu, S. (2007). Fluctuations of transfer RNAs between classical and hybrid states. Biophys J *93*, 3575-3582.

Lieberman, K.R., Firpo, M.A., Herr, A.J., Nguyenle, T., Atkins, J.F., Gesteland, R.F., and Noller, H.F. (2000). The 23 S rRNA environment of ribosomal protein L9 in the 50 S ribosomal subunit. J Mol Biol *297*, 1129-1143.

Marshall, R.A., Dorywalska, M., and Puglisi, J.D. (2008). Irreversible chemical steps control intersubunit dynamics during translation. Proc Natl Acad Sci U S A *105*, 15364-15369.

Munro, J.B., Altman, R.B., O'Connor, N., and Blanchard, S.C. (2007). Identification of two distinct hybrid state intermediates on the ribosome. Mol Cell *25*, 505-517.

Munro, J.B., Altman, R.B., Tung, C.S., Cate, J.H., Sanbonmatsu, K.Y., and Blanchard, S.C. (2010a). Spontaneous formation of the unlocked state of the ribosome is a multistep process. Proc Natl Acad Sci U S A *107*, 709-714.

Munro, J.B., Altman, R.B., Tung, C.S., Sanbonmatsu, K.Y., and Blanchard, S.C. (2010b). A fast dynamic mode of the EF-G-bound ribosome. EMBO J *29*, 770-781.

Munro, J.B., Wasserman, M.R., Altman, R.B., Wang, L., and Blanchard, S.C. (2010c). Correlated conformational events in EF-G and the ribosome regulate translocation. Nat Struct Mol Biol *17*, 1470-1477.

Qin, P., Yu, D., Zuo, X., and Cornish, P.V. (2014). Structured mRNA induces the ribosome into a hyper-rotated state. EMBO Rep *15*, 185-190.

Richter, D. (1976). Stringent factor from Escherichia coli directs ribosomal binding and release of uncharged tRNA. Proc Natl Acad Sci U S A *73*, 707-711.

Rodnina, M.V., Savelsbergh, A., Katunin, V.I., and Wintermeyer, W. (1997). Hydrolysis of GTP by elongation factor G drives tRNA movement on the ribosome. Nature *385*, 37-41.

Rodnina, M.V., and Wintermeyer, W. (1995). GTP consumption of elongation factor Tu during translation of heteropolymeric mRNAs. Proc Natl Acad Sci U S A *92*, 1945-1949.

Savelsbergh, A., Katunin, V.I., Mohr, D., Peske, F., Rodnina, M.V., and Wintermeyer, W. (2003). An elongation factor G-induced ribosome rearrangement precedes tRNA-mRNA translocation. Mol Cell *11*, 1517-1523.

Savelsbergh, A., Matassova, N.B., Rodnina, M.V., and Wintermeyer, W. (2000). Role of domains 4 and 5 in elongation factor G functions on the ribosome. J Mol Biol *300*, 951-961.

Wasserman, M.R., Alejo, J.L., Altman, R.B., and Blanchard, S.C. (2016). Multiperspective smFRET reveals rate-determining late intermediates of ribosomal translocation. Nat Struct Mol Biol *23*, 333-341.

Wohlgemuth, I., Brenner, S., Beringer, M., and Rodnina, M.V. (2008). Modulation of the rate of peptidyl transfer on the ribosome by the nature of substrates. J Biol Chem *283*, 32229-32235.